

Fidelity susceptibility and long-range correlation in the Kitaev honeycomb model

Shuo Yang,^{1,2} Shi-Jian Gu,^{1,*} Chang-Pu Sun,² and Hai-Qing Lin¹

¹*Department of Physics and ITP, The Chinese University of Hong Kong, Hong Kong, China*

²*Institute of Theoretical Physics, Chinese Academy of Sciences, Beijing, 100080, China*

(Dated: October 28, 2018)

We study exactly both the ground-state fidelity susceptibility and bond-bond correlation function in the Kitaev honeycomb model. Our results show that the fidelity susceptibility can be used to identify the topological phase transition from a gapped A phase with Abelian anyon excitations to a gapless B phase with non-Abelian anyon excitations. We also find that the bond-bond correlation function decays exponentially in the gapped phase, but algebraically in the gapless phase. For the former case, the correlation length is found to be $1/\xi = 2 \sinh^{-1}[\sqrt{2J_z - 1}/(1 - J_z)]$, which diverges around the critical point $J_z = (1/2)^+$.

PACS numbers: 03.67.-a, 64.60.-i, 05.30.Pr, 75.10.Jm

I. INTRODUCTION

Quite recently, a great deal of effort [1, 2, 3, 4, 5, 6, 7, 8, 9, 10, 11, 12, 13, 14, 15, 16] has been devoted to the role of fidelity, a concept borrowed from quantum information theory [17], in quantum phase transitions (QPTs) [18]. The motivation is quite obvious. Since the fidelity is a measure of similarity between two states, the change of the ground state structure around the quantum critical point should result in a dramatic change in the fidelity across the critical point. Such a fascinating prospect has been demonstrated in many correlated systems. For example, in the one-dimensional XY model, the fidelity shows a narrow trough at the phase transition point [2]. Similar properties were also found in fermionic [3] and bosonic systems [4]. The advantage of the fidelity is that, since the fidelity is a space geometrical quantity, no a priori knowledge of the order parameter and symmetry-breaking is required in studies of QPTs.

Nevertheless, the properties of the fidelity are mainly determined by its leading term [7, 8], i.e., its second derivative with respect to the driving parameter (or the so-called fidelity susceptibility [8]). According to the standard perturbation method, it has been shown that the fidelity susceptibility actually is equivalent to the structure factor (fluctuation) of the driving term in the Hamiltonian [8]. For example, if we focus on the thermal phase transitions and choose the temperature as the driving parameter, the fidelity susceptibility, extracted from the mixed state fidelity between two thermal states [6], is simply the specific heat [7, 8]. From this point of view, the fidelity approach to QPTs seems still to be within the framework of the correlation functions approach, which is intrinsically related to the local order parameter.

However, some systems cannot be described in a framework built on the local order parameter. This might be due to the absence of preexisting symmetry in the

Hamiltonian, such as topological phase transitions [19] and Kosterlitz-Thouless phase transitions [20]. For the latter, since the transition is of infinite-order, it has already been pointed out that the fidelity might fail to identify the phase transition point [8, 11]. Therefore, it is an interesting issue to address the role of fidelity in studying the topological phase transition.

The Kitaev honeycomb model was first introduced by Kitaev in search of topological order and anyonic statistics. The model is associated with a system of 1/2 spins which are located at the vertices of a honeycomb lattice. Each spin interacts with three nearest neighbor spins through three types of bonds, called “ $x(y, z)$ -bonds” depending on their direction. The model Hamiltonian [21] is as follows:

$$\begin{aligned} H &= -J_x \sum_{x\text{-bonds}} \sigma_j^x \sigma_k^x - J_y \sum_{y\text{-bonds}} \sigma_j^y \sigma_k^y - J_z \sum_{z\text{-bonds}} \sigma_j^z \sigma_k^z, \\ &= -J_x H_x - J_y H_y - J_z H_z. \end{aligned} \quad (1)$$

where j, k denote the two ends of the corresponding bond, and J_a, σ^a ($a = x, y, z$) are dimensionless coupling constants and Pauli matrices respectively. Such a model is rather artificial. However, its potential application in topological quantum computation has made it a focus of research in recent years [21, 22, 23, 24, 25, 26, 27, 28, 29, 30, 31, 32].

The ground state of the Kitaev honeycomb model consists of two phases, i.e., a gapped A phase with Abelian anyon excitations and a gapless B phase with non-Abelian anyon excitations. The transition has been studied by various approaches. For example, it has been shown that a kind of long range order exists in the dual space [26], such that basic concepts of Landau’s theory of continuous phase transitions might still be applied. In real space, however, the spin-spin correlation functions vanishes rapidly with increasing distance between two spins. Therefore, the transition between the two phases is believed to be of topological type due to the absence of a local order parameter in real space [21].

In this work, we *firstly* try to investigate the topological QPT occurring in the ground state of the Kitaev

*Electronic address: sjgu@phy.cuhk.edu.hk

honeycomb model in terms of the fidelity susceptibility. We find that the fidelity susceptibility can be used to identify the topological phase transition from a gapped phase with Abelian anyon excitations to gapless phase with non-Abelian anyon excitations. Various scaling and critical exponents of the fidelity susceptibility around the critical points are obtained through a standard finite-size scaling analysis. *These observations from the fidelity approach are a little surprising.* Our earlier thought was that the fidelity susceptibility, which is a kind of structure factor obtained by a combination of correlation functions, can hardly be related to the topological phase transition, since the latter cannot be described by the correlation functions of local operators. So our *second* motivation following from the first one is to study the dominant correlation function appearing in the definition of the fidelity susceptibility, i.e., the bond-bond correlation function. We find that the correlation function decays algebraically in the gapless phase, but exponentially in the gapped phase. For the latter, the correlation length takes the form $1/\xi = 2 \sinh^{-1}[\sqrt{2J_z - 1}/(1 - J_z)]$ along a given evolution line. Therefore, the divergence of the correlation length around the critical point $J_z = (1/2)^+$ is also a signature of the QPT.

We organize our work as follows. In Sec. II, we introduce briefly the definition of the fidelity susceptibility in the Hamiltonian parameter space, then we diagonalize the Hamiltonian based on Kitaev's approaches and obtain the explicit forms of the Riemann metric tensor, from which the fidelity susceptibility along any direction can be obtained. The critical and scaling behaviors of the fidelity susceptibility are also studied numerically. In Sec. III, we explicitly calculate the bond-bond correlation functions in both phases. Its long range behavior and the correlation length in the gapped phase are studied both analytically and numerically. Sec. IV includes a brief summary.

II. FIDELITY SUSCEPTIBILITY IN THE GROUND STATE

To study the fidelity susceptibility, we notice that the structure of the parameter space of the Hamiltonian (1) is three dimensional. In this space, we can always let the ground state of the Hamiltonian evolves along a certain path in the parameter space, i.e.,

$$J_a = J_a(\lambda), \quad (2)$$

where λ is a kind of driving parameter along the evolution line. We then extend the definition of fidelity to this arbitrary line in high-dimensional space. Following Ref. [2], the fidelity is defined as the overlap between two ground states

$$F = |\langle \Psi_0(\lambda) | \Psi_0(\lambda + \delta\lambda) \rangle|, \quad (3)$$

where $\delta\lambda$ is the magnitude of a small displacement along the tangent direction at λ . Then the fidelity susceptibil-

ity along this line can be calculated as

$$\chi_F = \lim_{\delta\lambda \rightarrow 0} \frac{-2 \ln F_i}{\delta\lambda^2} = \sum_{ab} g_{ab} n^a n^b, \quad (4)$$

where $n^a = \partial J_a / \partial \lambda$ denotes the tangent unit vector at the given point, and g_{ab} is the Riemann metric tensor introduced by Zanardi, Giorda, and Cozzini[7]. For the present model, we have

$$g_{ab} = \sum_n \frac{\langle \Psi_n(\lambda) | H_a | \Psi_0(\lambda) \rangle \langle \Psi_0(\lambda) | H_b | \Psi_n(\lambda) \rangle}{(E_n - E_0)^2}, \quad (5)$$

where $|\Psi_n(\lambda)\rangle$ is the eigenstate of the Hamiltonian with energy E_n . Clearly, g_{ab} does not depend on the specific path along which the system evolves. However, once g_{ab} are obtained, the fidelity susceptibility is just a simple combination of g_{ab} together with a unit vector which defines the direction of system evolution in the parameter space.

According to Kitaev [21], the Hamiltonian (1) can be diagonalized exactly by introducing Majorana fermion operators to represent the Pauli operators as

$$\sigma^x = ib^x c, \quad \sigma^y = ib^y c, \quad \sigma^z = ib^z c, \quad (6)$$

where the Majorana operators satisfy $A^2 = 1$, $AB = -BA$ for $A, B \in \{b^x, b^y, b^z, c\}$ and $A \neq B$, and also $b^x b^y b^z c |\psi\rangle = |\psi\rangle$ to ensure the commutation relations of spin operators. Then the Hamiltonian can be written as

$$H = \frac{i}{2} \sum_{j,k} \hat{u}_{jk} J_{a_{jk}} c_j c_k. \quad (7)$$

Since the operators $\hat{u}_{jk} = ib_j^{a_{jk}} b_k^{a_{jk}}$ satisfy $[\hat{u}_{jk}, H] = 0$, $[\hat{u}_{jk}, \hat{u}_{ml}] = 0$, and $\hat{u}_{jk}^2 = 1$, they can be regarded as generators of the Z_2 symmetry group. Therefore, the whole Hilbert space can be decomposed into common eigenspaces of \hat{u}_{jk} , each subspace is characterized by a group of $u_{jk} = \pm 1$. The spin model is transformed to a quadratic Majorana fermionic Hamiltonian

$$H = \frac{i}{2} \sum_{j,k} u_{jk} J_{a_{jk}} c_j c_k. \quad (8)$$

Here we restrict ourselves to only the vortex free subspace with translational invariants, i.e., all $u_{jk} = 1$. After Fourier transformation, we get the Hamiltonian of a unit cell in the momentum representation [21],

$$H = \sum_{\mathbf{q}} \begin{pmatrix} a_{-\mathbf{q},1} \\ a_{-\mathbf{q},2} \end{pmatrix}^T \begin{pmatrix} 0 & \text{if}(\mathbf{q}) \\ -\text{if}(\mathbf{q})^* & 0 \end{pmatrix} \begin{pmatrix} a_{\mathbf{q},1} \\ a_{\mathbf{q},2} \end{pmatrix}, \quad (9)$$

where $\mathbf{q} = (q_x, q_y)$,

$$a_{\mathbf{q},\gamma} = \frac{1}{\sqrt{2L^2}} \sum_{\mathbf{r}} e^{-i\mathbf{q}\cdot\mathbf{r}} c_{\mathbf{r},\gamma}, \quad (10)$$

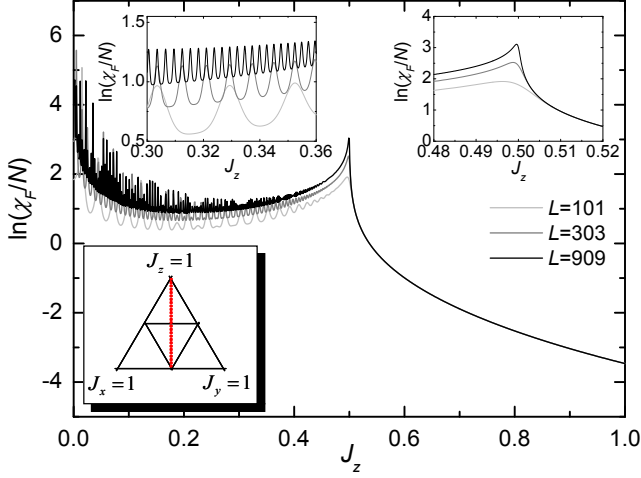


FIG. 1: (Color online) Fidelity susceptibility as a function of J_z along the dashed line shown in the triangle for various system sizes $L = 101, 303, 909$. Both upper insets correspond to enlarged pictures of two small portions.

\mathbf{r} refers to the coordinate of a unit cell, γ to a position type inside the cell, and

$$\begin{aligned} f(\mathbf{q}) &= \epsilon_{\mathbf{q}} + i\Delta_{\mathbf{q}}, \\ \epsilon_{\mathbf{q}} &= J_x \cos q_x + J_y \cos q_y + J_z, \\ \Delta_{\mathbf{q}} &= J_x \sin q_x + J_y \sin q_y. \end{aligned} \quad (11)$$

Here, we set L to be an odd integer, then the system size is $N = 2L^2$. The momenta take the values

$$q_{x(y)} = \frac{2n\pi}{L}, n = -\frac{L-1}{2}, \dots, \frac{L-1}{2}. \quad (12)$$

The above Hamiltonian can be rewritten using fermionic operators as

$$H = \sum_{\mathbf{q}} \sqrt{\epsilon_{\mathbf{q}}^2 + \Delta_{\mathbf{q}}^2} \left(C_{\mathbf{q},1}^\dagger C_{\mathbf{q},1} - C_{\mathbf{q},2}^\dagger C_{\mathbf{q},2} \right). \quad (13)$$

Therefore, we have the ground state

$$\begin{aligned} |\Psi_0\rangle &= \prod_{\mathbf{q}} C_{\mathbf{q},2}^\dagger |0\rangle \\ &= \prod_{\mathbf{q}} \frac{1}{\sqrt{2}} \left(\frac{\sqrt{\epsilon_{\mathbf{q}}^2 + \Delta_{\mathbf{q}}^2}}{\Delta_{\mathbf{q}} + i\epsilon_{\mathbf{q}}} a_{-\mathbf{q},1} + a_{-\mathbf{q},2} \right) |0\rangle, \end{aligned} \quad (14)$$

with the ground state energy

$$E_0 = - \sum_{\mathbf{q}} \sqrt{\epsilon_{\mathbf{q}}^2 + \Delta_{\mathbf{q}}^2}. \quad (15)$$

The fidelity of the two ground states at λ and λ' can be obtained as

$$\begin{aligned} F^2 &= \prod_{\mathbf{q}} \frac{1}{2} \left(1 + \frac{\Delta_{\mathbf{q}} \Delta'_{\mathbf{q}} + \epsilon_{\mathbf{q}} \epsilon'_{\mathbf{q}}}{E_{\mathbf{q}} E'_{\mathbf{q}}} \right), \\ &= \prod_{\mathbf{q}} \cos^2(\theta_{\mathbf{q}} - \theta'_{\mathbf{q}}). \end{aligned} \quad (16)$$

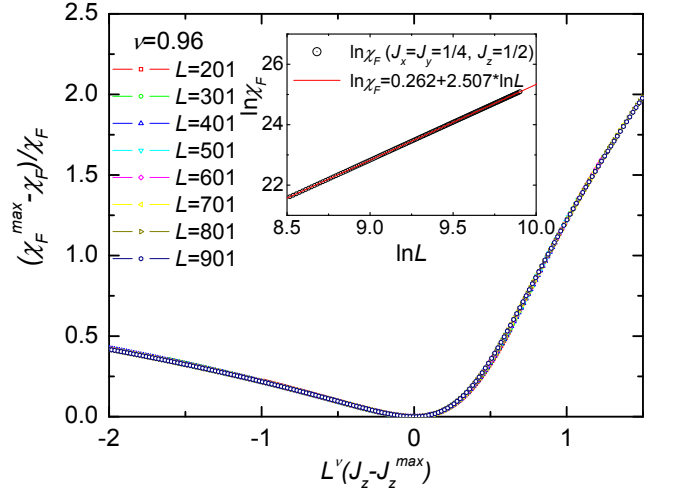


FIG. 2: (Color online) Finite size scaling analysis for the case of power-law divergence for system sizes $L = 201, 301, \dots, 901$. The fidelity susceptibility, considered as a function of system size and driving parameter is a function of $L^\nu(J_z - J_z^{\max})$ only, and has the critical exponent $\nu = 0.96$.

with

$$\begin{aligned} \cos(2\theta_{\mathbf{q}}) &= \frac{\epsilon_{\mathbf{q}}}{E_{\mathbf{q}}}, \sin(2\theta_{\mathbf{q}}) = \frac{\Delta_{\mathbf{q}}}{E_{\mathbf{q}}}, \\ \cos(2\theta'_{\mathbf{q}}) &= \frac{\epsilon'_{\mathbf{q}}}{E'_{\mathbf{q}}}, \sin(2\theta'_{\mathbf{q}}) = \frac{\Delta'_{\mathbf{q}}}{E'_{\mathbf{q}}}. \end{aligned} \quad (17)$$

The Riemann metric tensor can be expressed as

$$g^{ab} = \sum_{\mathbf{q}} \left(\frac{\partial \theta_{\mathbf{q}}}{\partial J_a} \right) \left(\frac{\partial \theta_{\mathbf{q}}}{\partial J_b} \right), \quad (18)$$

where

$$\begin{aligned} \frac{\partial(2\theta_{\mathbf{q}})}{\partial J_x} &= \frac{J_z \sin q_x + J_y \sin(q_x - q_y)}{\epsilon_{\mathbf{q}}^2 + \Delta_{\mathbf{q}}^2} \cdot \frac{\Delta_{\mathbf{q}}}{|\Delta_{\mathbf{q}}|}, \\ \frac{\partial(2\theta_{\mathbf{q}})}{\partial J_y} &= -\frac{J_x \sin(q_x - q_y) - J_z \sin q_y}{\epsilon_{\mathbf{q}}^2 + \Delta_{\mathbf{q}}^2} \cdot \frac{\Delta_{\mathbf{q}}}{|\Delta_{\mathbf{q}}|}, \\ \frac{\partial(2\theta_{\mathbf{q}})}{\partial J_z} &= -\frac{J_x \sin q_x + J_y \sin q_y}{\epsilon_{\mathbf{q}}^2 + \Delta_{\mathbf{q}}^2} \cdot \frac{\Delta_{\mathbf{q}}}{|\Delta_{\mathbf{q}}|}. \end{aligned} \quad (19)$$

Clearly, with these equations, we can in principle calculate the fidelity susceptibility along any direction in the parameter space according to Eq. (4). Here, we would like to point out that the same results can be obtained from the generalized Jordan-Wigner transformation used firstly by Feng, Zhang, and Xiang[26].

Following Kitaev [21], we restrict our studies to the plane $J_x + J_y + J_z = 1$ (see the large triangle in Fig. 1). According to his results, the plane consists of two phases, i.e., a gapped A phase with Abelian anyon excitations and a gapless B phase with non-Abelian excitations. The two phases are separated by three transition lines, i.e. $J_x = 1/2$, $J_y = 1/2$, and $J_z = 1/2$ which form a small triangle in the B phase.

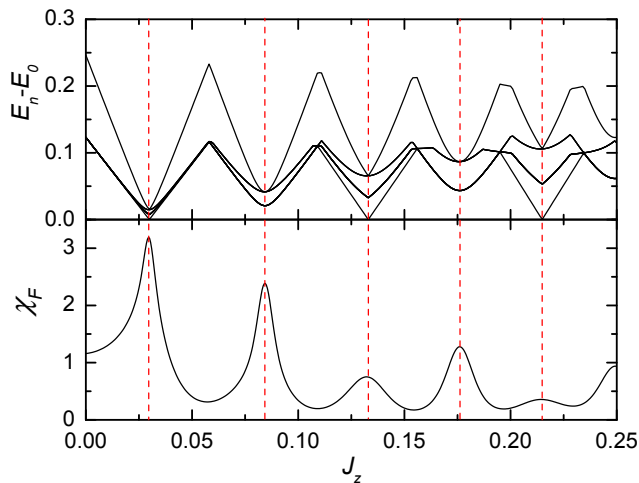


FIG. 3: (Color online) Fidelity susceptibility and a few low-lying excitations as a function of J_z in a small portion of the evolution line for system size $L = 51$.

Generally, we can define an arbitrary evolution line on the plane. Without loss of generality, we first choose the line as $J_x = J_y$ (see the dashed line in the triangle of Fig. 1). Then the fidelity susceptibility along this line can be simplified as

$$\chi_F = \frac{1}{16} \sum_{\mathbf{q}} \left[\frac{\sin q_x + \sin q_y}{\epsilon_{\mathbf{q}}^2 + \Delta_{\mathbf{q}}^2} \right]^2. \quad (20)$$

The numerical results of different system sizes are shown in Fig. 1. First of all, the fidelity susceptibility per site, i.e. χ_F/N diverges quickly with increasing system size around the critical point $J_z = 1/2$. This property is similar to the fidelity susceptibility in other systems, such as the one-dimensional Ising chain [2] and the asymmetric Hubbard model [12]. Secondly, χ_F/N is an intensive quantity in the A phase ($J_z > 1/2$), while in the B phase, the fidelity susceptibility also diverges with increasing system size. Thirdly, the fidelity susceptibility shows many peaks in the B phase, the number of peaks increases linearly with the system size L (see the left upper inset of Fig. 1). The phenomena of fidelity susceptibility per site in the B phase have not been found in other systems previously, to our knowledge, so that they are rather impressive.

To study the scaling behavior of the fidelity susceptibility around the critical point, we perform a finite-size scaling analysis. Since the fidelity susceptibility in the A phase is an intensive quantity, the fidelity susceptibility in the thermodynamic limit, scales as [12]

$$\frac{\chi_F}{N} \propto \frac{1}{|J_z - J_z^c|^\alpha}. \quad (21)$$

around $J_z^c = 1/2$. Meanwhile, the maximum point of χ_F at $J_z = J_z^{\max}$ for a finite sample behaves as

$$\frac{\chi_F}{N} \propto L^\mu, \quad (22)$$

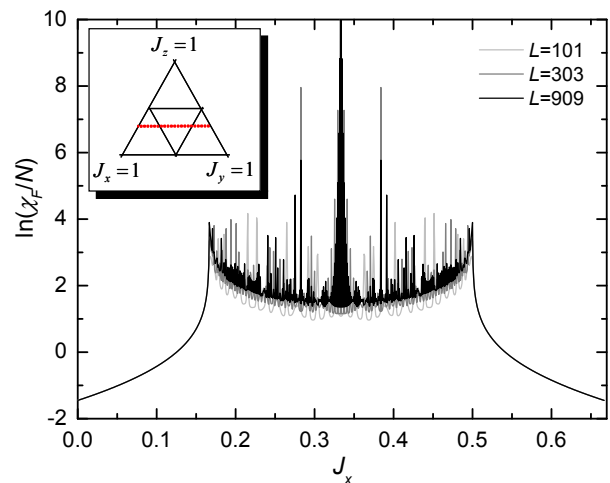


FIG. 4: (Color online) Fidelity susceptibility as a function of $J_x = 2/3 - J_y$ along the dashed line shown in the triangle for various system sizes $L = 101, 303, 909$.

with $\mu = 0.507 \pm 0.0001$ (see the inset of Fig. 2). According to the scaling ansatz, the rescaled fidelity susceptibility around its maximum point at J_z^{\max} is just a simple function of the rescaled driving parameter, i.e.,

$$\frac{\chi_F^{\max} - \chi_F}{\chi_F} = f[L^\nu (J_z - J_z^{\max})]. \quad (23)$$

where $f(x)$ is a universal scaling function and does not depend on the system size, and ν is the critical exponent. The function $f(x)$ is shown in Fig. 2. Clearly, the rescaled fidelity susceptibilities of various system sizes fall onto a single line for a specific $\nu = 0.96 \pm 0.005$. Then the critical exponent α can be obtained as

$$\alpha = \frac{\mu}{\nu} = 0.528 \pm 0.001. \quad (24)$$

One of the most interesting observations is that a huge number of peaks appear in the B phase. The scaling analysis shows that the number of peaks is proportional to the system size. Physically, a peak means that the ground state can not adiabatically evolve from one side of the peak to the other side easily because the two ground states have distinct features. From this point of view, the ground state in the B phase might be stable to an adiabatic perturbation. Moreover, the existence of many peaks can also be reflected by reconstruction of the energy spectra. For this purpose, we choose a small portion of the evolution line and plot both the fidelity susceptibility and a few low-lying excitations in Fig. 3. Since the fidelity is inversely proportional to the energy gap [Eq. (5)], the location of each peak corresponds to a gap minimum.

Similarly, we can also choose the system evolution line as $J_z = 1/3$, the fidelity susceptibility then takes the form

$$\chi_F = \frac{1}{36} \sum_{\mathbf{q}} \left[\frac{(\sin q_x - \sin q_y) + 2 \sin(q_x - q_y)}{\epsilon_{\mathbf{q}}^2 + \Delta_{\mathbf{q}}^2} \right]^2. \quad (25)$$

The numerical results for this case are shown in Fig. 4. The results are qualitatively similar to those of previous cases. In the B phase, there still exist many peaks. Both the number and the magnitude of the peaks increase with the system size, while in the A phase, the fidelity susceptibility becomes an intensive quantity.

III. LONG-RANGE CORRELATION AND FIDELITY SUSCEPTIBILITY

Follow You, *et al.* [8], the fidelity susceptibility is a combination of correlation functions. Precisely, for a general Hamiltonian

$$H = H_0 + \lambda H_I, \quad (26)$$

the fidelity susceptibility can be calculated as

$$\chi_F = \int \tau [\langle \Psi_0 | H_I(\tau) H_I(0) | \Psi_0 \rangle - \langle \Psi_0 | H_I | \Psi_0 \rangle^2] d\tau, \quad (27)$$

with τ being the imaginary time and

$$H_I(\tau) = e^{H(\lambda)\tau} H_I e^{-H(\lambda)\tau}.$$

Therefore, the divergence of the fidelity susceptibility at the critical point implies the existence of a long-range correlation function. Without loss of generality, if we still restrict ourselves to the plane $J_x + J_y + J_z = 1$ and choose J_z ($J_x = J_y$) as the driving parameter, the bond-bond correlation function is defined as

$$C(\mathbf{r}_1, \mathbf{r}_2) = \langle \sigma_{\mathbf{r}_1,1}^z \sigma_{\mathbf{r}_1,2}^z \sigma_{\mathbf{r}_2,1}^z \sigma_{\mathbf{r}_2,2}^z \rangle - \langle \sigma_{\mathbf{r}_1,1}^z \sigma_{\mathbf{r}_1,2}^z \rangle \langle \sigma_{\mathbf{r}_2,1}^z \sigma_{\mathbf{r}_2,2}^z \rangle. \quad (28)$$

Here the subscripts $\mathbf{r}_1, 1$ and $\mathbf{r}_1, 2$ denote the two ends of the single z -bond at $\mathbf{r}_1 = (x, y)$. In the vortex-free case, through Eqs. (6), (10), and (14), the spin operators $\sigma_{\mathbf{r}_1,1}^z \sigma_{\mathbf{r}_1,2}^z$ can be expressed in the form of fermion operators. So we finally get

$$\langle \sigma_{\mathbf{r}_1,1}^z \sigma_{\mathbf{r}_1,2}^z \rangle = \langle \sigma_{\mathbf{r}_2,1}^z \sigma_{\mathbf{r}_2,2}^z \rangle = \frac{1}{N} \sum_{\mathbf{q}} \frac{\epsilon_{\mathbf{q}}}{E_{\mathbf{q}}} \quad (29)$$

and

$$\begin{aligned} & \langle \Psi_0 | \sigma_{\mathbf{r}_1,1}^z \sigma_{\mathbf{r}_1,2}^z \sigma_{\mathbf{r}_2,1}^z \sigma_{\mathbf{r}_2,2}^z | \Psi_0 \rangle \\ &= \frac{1}{N^2} \sum_{\mathbf{q}, \mathbf{q}'} \{ \cos [(\mathbf{q} - \mathbf{q}') \cdot (\mathbf{r}_1 - \mathbf{r}_2)] - 1 \} \\ & \quad \times \frac{(\Delta_{\mathbf{q}} \Delta_{\mathbf{q}'} - \epsilon_{\mathbf{q}} \epsilon_{\mathbf{q}'})}{E_{\mathbf{q}} E_{\mathbf{q}'}} \end{aligned} \quad (30)$$

with $\mathbf{q} \neq \mathbf{q}'$ and $\mathbf{r}_1 \neq \mathbf{r}_2$. The same results can also be obtained by using the Jordan-Wigner transformation method [26, 27].

We show the dependence of the correlation function Eq. (28) on the distance for a finite sample of $L = 100$ in Fig. 5. Obviously, the lines can be divided into two

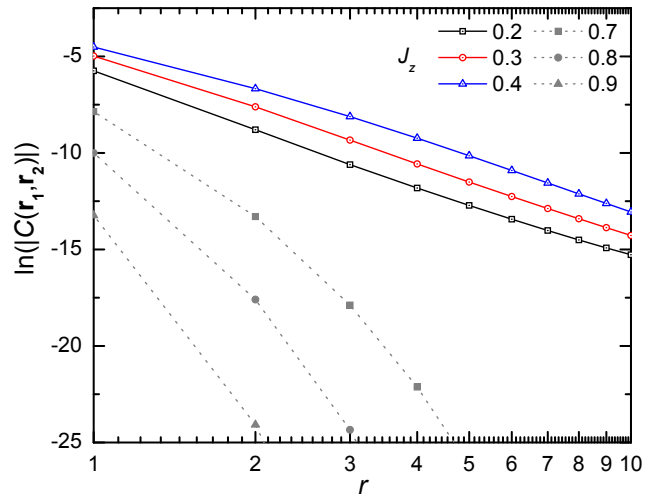


FIG. 5: (Color online) Bond-bond correlation function as a function of distance r for various J_z and a finite sample of $L = 100$, where $\mathbf{r}_1 - \mathbf{r}_2 = (r, r)$. Downward peaks in top lines are due to zero-point crossing.

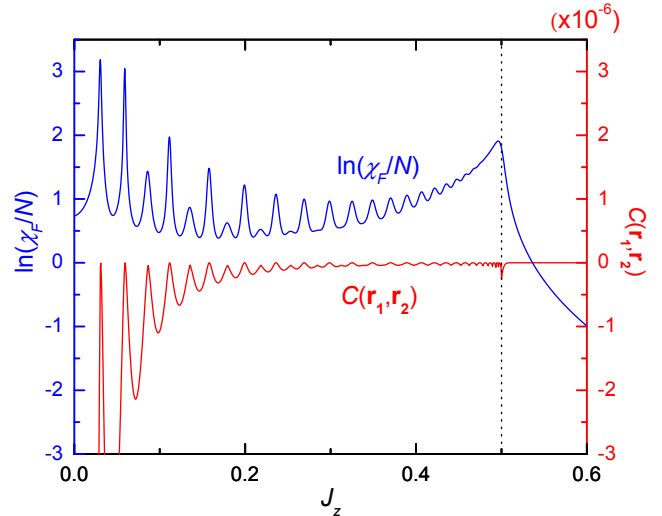


FIG. 6: (Color online) Fidelity susceptibility and the correlation function at $\mathbf{r}_1 - \mathbf{r}_2 = (L/2, L/2)$ as a function of J_z for a finite sample of $L = 100$.

groups. In the gapless phase ($J_z < 1/2$), the correlation function decays algebraically, while in the gapped phase ($J_z > 1/2$), it decays exponentially. If $J_z < 1/2$, the denominator in Eq. (30) has two zero points, which are of order $1/N$ in the large N limit. Their contribution causes the summation to be finite in the thermodynamic limit. Then using the stationary phase method, we can evaluate the exponents of the correlation function at long distance to be 4, i.e.,

$$C(\mathbf{r}_1, \mathbf{r}_2) \propto \frac{1}{|\mathbf{r}_1 - \mathbf{r}_2|^4}. \quad (31)$$

From Fig. 5, the average slope of the top three lines

around $r = 10$ is estimated to be 4.05, which is slightly different from 4. Nevertheless, we would rather interpret the difference as due to both finite size effects and numerical error. On the other hand, if $J_z > 1/2$, the phase is gapped and the denominator in Eq. (30) does not have zero point on the real axis. Therefore, the whole summation is strongly suppressed except for the case of small $|\mathbf{r}_1 - \mathbf{r}_2|$, whose range actually defines the correlation length. In order to evaluate the correlation, we need to extend the integrand (in the thermodynamic limit) in Eq. (30) to the whole complex plane, where we can find two singular points. Using the steepest descent method, we can evaluate the correlation length to be

$$\frac{1}{\xi} = 2 \sinh^{-1} \frac{\sqrt{2J_z - 1}}{1 - J_z}. \quad (32)$$

Obviously, the correlation length becomes divergent as $J_z \rightarrow 0.5^+$. This property can also be used to signal the QPT occurring in the Kitaev honeycomb model in addition to the fidelity and Chern number [21]. The correlation length we obtained is the same as that of the string operators [27], which, however, is a non-local operator.

Although it is not easy to calculate the fidelity susceptibility from the correlation function directly due to the dynamic term in Eq. (27), our conjecture is confirmed for the present model. That is the divergence of the fidelity susceptibility is related to the long-range correlations. Fig. 6 is illustrative. The correlation function at $\mathbf{r}_1 - \mathbf{r}_2 = (L/2, L/2)$, in spite of its smallness, remains nonzero in the region $J_z < 1/2$, but it vanishes in $J_z > 1/2$. For the former, the oscillating structures of the two lines meet each other.

IV. SUMMARY AND DISCUSSION

In summary, we have studied the critical behavior of the fidelity susceptibility where a topological phase tran-

sition occurs in the honeycomb Kitaev model. Though no symmetry breaking exists and no local order parameter in real space can be used to describe the transition, the fidelity susceptibility definitely can indicate the transition point. We found that the fidelity susceptibility per site is an intensive quantity in the gapped phase, while in the gapless phase, the huge number of peaks reflects frequent spectral reconstruction along the evolution line. We also studied various scaling and critical exponents of the fidelity susceptibility around the critical points.

Based on the conclusions from the fidelity, we further studied the bond-bond correlation function in both phases. We found that the bond-bond correlation function, which plays a dominant role in the expression for the fidelity susceptibility, decays exponentially in the gapped phase, but algebraically in the gapless phase. The critical exponents of the correlation function in both the gapless and gapped phases are calculated numerical and analytically. Therefore, in addition to the topological properties of the Kitaev honeycomb model, say, the Chern number, we found that both the fidelity susceptibility and the bond-bond correlation functions can be used to witness the QPT in the model.

Note added. After finishing this work, we noticed that a work on the fidelity per site instead of the fidelity susceptibility in a similar model appeared[33].

Acknowledgments

We thank Xiao-Gang Wen, Yu-Peng Wang, Guang-Ming Zhang, and Jun-Peng Cao for helpful discussions. This work is supported by CUHK (Grant No. A/C 2060344) and NSFC.

-
- [1] H. T. Quan, Z. Song, X. F. Liu, P. Zanardi, and C. P. Sun, Phys. Rev. Lett. **96**, 140604 (2006).
 - [2] P. Zanardi and N. Paunkovic, Phys. Rev. E **74**, 031123 (2006).
 - [3] P. Zanardi, M. Cozzini, and P. Giorda, J. Stat. Mech. L02002 (2007); M. Cozzini, P. Giorda, and P. Zanardi, Phys. Rev. B **75**, 014439 (2007); M. Cozzini, R. Ionicioiu, and P. Zanardi, Phys. Rev. B **76**, 104420 (2007).
 - [4] P. Buonsante and A. Vezzani, Phys. Rev. Lett. **98**, 110601 (2007).
 - [5] P. Zanardi, H. T. Quan, X. Wang, and C. P. Sun, Phys. Rev. A **75**, 032109 (2007).
 - [6] P. Zanardi, H. T. Quan, X. G. Wang, and C. P. Sun, Phys. Rev. A **75**, 032109 (2007).
 - [7] P. Zanardi, P. Giorda, and M. Cozzini, Phys. Rev. Lett. **99**, 100603 (2007).
 - [8] W. L. You, Y. W. Li, and S. J. Gu, Phys. Rev. E **76**, 022101 (2007).
 - [9] H. Q. Zhou and J. P. Barjaktarevic, arXiv: cond-mat/0701608; H. Q. Zhou, J. H. Zhao, and B. Li, arXiv:0704.2940;
 - [10] L. C. Venuti and P. Zanardi, Phys. Rev. Lett. **99**, 095701 (2007).
 - [11] S. Chen, L. Wang, S. J. Gu, and Y. Wang, Phys. Rev. E **76** 061108 (2007); S. Chen, L. Wang, Y. Hao, and Y. Wang, arXiv:0801.0020.
 - [12] S. J. Gu, H. M. Kwok, W. Q. Ning, and H. Q. Lin, arXiv:0706.2495.
 - [13] M. F. Yang, Phys. Rev. B **76**, 180403 (R) (2007); Y. C. Tzeng and M. F. Yang, Phys. Rev. A **77**, 012311 (2008).
 - [14] N. Paunkovic, P. D. Sacramento, P. Nogueira, V. R. Vieira, and V. K. Dugaev, arXiv:0708.3494.
 - [15] H. Q. Zhou, R. Orus, and G. Vidal, Phys. Rev. Lett. **100** 080601 (2008).

- [16] A. Hamma, W. Zhang, S. Haas, and D. A. Lidar, arXiv:0705.0026.
- [17] M. A. Nilesen and I. L. Chuang, *Quantum Computation and Quantum Information* (Cambridge University Press, Cambridge, England, 2000).
- [18] S. Sachdev, *Quantum Phase Transitions* (Cambridge University Press, Cambridge, England, 1999).
- [19] X. G. Wen, *Quantum Field Theory of Many-Body Systems* (Oxford University, New York, 2004).
- [20] J. M. Kosterlitz and D. J. Thouless, *J. Phys. C* **6**, 1181(1973).
- [21] A. Kitaev, *Ann. Phys.* **303**, 2 (2003); *Ann. Phys.* **321**, 2 (2006).
- [22] X. G. Wen, *Phys. Rev. Lett.* **90**, 016803 (2003); M. A. Levin and X. G. Wen, *Phys. Rev. B* **71**, 045110 (2005).
- [23] J. Preskill, *Topological quantum computation*, <http://www.theory.caltech.edu/people/preskill/ph229/> (2004).
- [24] J. K. Pachos, *IJQI* **4**, 947 (2006); *Ann. Phys.* **322**, 1254 (2007).
- [25] S. D. Sarma, M. Freedman, C. Nayak, S. H. Simon, A. Stern, *Rev. Mod. Phys.*, accepted.
- [26] X. Y. Feng, G. M. Zhang, and T. Xiang, *Phys. Rev. Lett.* **98**, 087204 (2007); D. H. Lee, G. M. Zhang, and T. Xiang, *Phys. Rev. Lett.* **99**, 196805 (2007).
- [27] H. D. Chen and J. P. Hu, arXiv: cond-mat/0702366; H. D. Chen and Z. Nussinov, *J. Phys. A: Math. Theor.* **41**, 075001 (2008); Z. Nussinov, G. Ortiz, arXiv: cond-mat/0702377.
- [28] Y. Yu, arXiv: 0704.3829; Y. Yu, Z. Q. Wang, arXiv: 0708.0631; T. Y. Si and Y. Yu, arXiv:0709.1302; T. Y. Si and Y. Yu, arXiv: 0712.4231 .
- [29] S. Yang, D. L. Zhou, and C. P. Sun, *Phys. Rev. B* **76**, 180404(R) (2007).
- [30] S. P. Kou and X. G. Wen, arXiv: 0711.0571.
- [31] S. Mandal and N. Surendran, arXiv: 0801.0229.
- [32] K. P. Schmidt, S. Dusuel, and J. Vidal, *Phys. Rev. Lett.* **100**, 057208 (2008); S. Dusuel, K. P. Schmidt, and J. Vidal, arXiv:0802.0379.
- [33] J. H. Zhao and H. Q. Zhou, arXiv:0803.0814.